Original Article

Applying the AAPM 293 report to estimate the absorbed dose during head computed tomography: using head circumference for rapid dose estimation

Tiao Chen[1#], Xiangchuang Kong[2,3#], Wei Peng[1], Tian Liao[2,3], Huaifei Hu[4], Ning Pan[4,5*], Zilong Yuan[1*]

[1]Department of Radiology, Hubei Cancer Hospital, Tongji Medical College, Huazhong University of Science and Technology, Wuhan, China; [2]Department of Radiology, Union Hospital, Tongji Medical College, Huazhong University of Science and Technology, Wuhan, China; [3]Hubei Province Key Laboratory of Molecular Imaging, Wuhan, China; [4]College of Biomedical Engineering, South-Central Minzu University, Wuhan, China; [5]Hubei Province Key Laboratory of Medical Information Analysis and Tumor Diagnosis & Treatment, Wuhan, China

Contributions: (I) Conception and design: T Chen, Z Yuan, N Pan; (II) Administrative support: X Kong, H Hu, N Pan; (III) Provision of study materials or patients: T Chen, X Kong, W Peng, T Liao, Z Yuan; (IV) Collection and assembly of data: T Chen, X Kong, W Peng, T Liao, Z Yuan; (V) Data analysis and interpretation: T Chen, X Kong, N Pan, Z Yuan; (VI) Manuscript writing: All authors; (VII) Final approval of manuscript: All authors.

[#]These authors contributed equally to this work and should be considered as co-first authors.

[*]These authors contributed equally to this work and should be considered as co-corresponding authors.

Correspondence to: Zilong Yuan. Department of Radiology, Hubei Cancer Hospital, Tongji Medical College, Huazhong University of Science and Technology, No. 116 Zhuodaoquan South Road, Hongshan District, Wuhan 430079, China. Email: yuanzilong0213@126.com; Ning Pan. College of Biomedical Engineering, South-Central Minzu University, No. 182 National Avenue, Hongshan District, Wuhan 430079, China. Email: panning@mail.scuec.edu.cn.

Background: The American Association of Physicists in Medicine (AAPM) report 293 is more accurate than report 220 in evaluating the absorbed radiation dose during head computed tomography (CT) examination. We aimed to investigate the associations between age, head circumference (HC), the conversion factor (f_{293}), and specific-size dose estimation ($SSDE_{293}$) during these procedures. The rapid radiation dose was also estimated based on the AAPM report 293.

Methods: In this retrospective, cross-sectional study, unenhanced CT images of the head were retrospectively collected from 1,222 participants from Union Hospital and Hubei Cancer Hospital between December 2018 and September 2019. Scan parameters, including age, HC, water-equivalent diameter (D_W), and volumetric computed tomography dose index ($CTDI_{vol}$), were generated automatically using indigenously-developed image processing software. The corresponding f_{293} and $SSDE_{293}$ were calculated according to the AAPM report 293. The analyses were performed using linear regression.

Results: In the younger group, age and HC were significantly negatively correlated with $SSDE_{293}$ (r=–0.33 and –0.44, respectively; both P values ≤0.001). No significant correlation was reported between age, HC, and $SSDE_{293}$ in the older group. Moreover, age was significantly negatively associated with f_{293} in the younger and older groups (r=–0.80 and –0.13, respectively; both P values ≤0.001). A significantly negative association was seen between f_{293} and increased HC in both age groups (r=–0.92 and –0.82, respectively; both P values ≤0.001).

Conclusions: The HC of patients was associated with head conversion. HC is a feasible indicator for rapidly estimating the radiation dose in head CT examinations based on the AAPM report 293.

Keywords: Computed tomography (CT); water-equivalent diameter (D_W); head circumference (HC); size-specific dose estimate (SSDE)

Submitted Sep 18, 2022. Accepted for publication Mar 02, 2023. Published online Mar 10, 2023.
doi: 10.21037/qims-22-983
View this article at: https://dx.doi.org/10.21037/qims-22-983

Introduction

Emerging evidence demonstrates a patient's absorbed dose depends on the computed tomography (CT) scanner radiation dose output during CT examinations (1-3). The most common scanner output dose metrics for CT systems are the volumetric CT dose index ($CTDI_{vol}$) and dose-length product (DLP) (4,5). $CTDI_{vol}$ and DLP indicate the absorbed dose of polymethyl methacrylate (PMMA) phantoms with defined diameters of 16 and 32 cm for the head and body, respectively (6-9). However, $CTDI_{vol}$ and DLP do not represent the actual absorbed patient dose, as they do not account for patient size (10,11). The American Association of Physicists in Medicine (AAPM) aimed to improve the accuracy of patient dose estimation by proposing a formula to calculate the size-specific dose estimate (SSDE) (12,13), and in 2019 issued report 293 to estimate the dose for head CT examinations (14). While this and AAPM report 220 rely on similar calculation methods, the conversion factor (*f*) of report 293 is more accurate because its calculation method is based on head phantom experiments that consider different ages and the Monte Carlo simulation (15). A recent study also showed the average local SSDE calculated using size conversion factors from the AAPM report 293 has the highest accuracy for estimating eye lens radiation doses (16).

Conventionally, the water-equivalent diameter (D_W) used to calculate SSDE is executed after scanning ($f = \alpha e^{-\beta D_W}$, where f is the conversion factor and α and β are constants) (12). However, this approach is tedious and unsuitable for rapidly estimating the radiation dose in a busy CT center (17). Studies have shown that several parameters, including patient weight and body mass index (BMI), can be applied to rapidly estimate SSDE (17,18), although Alikhani *et al.* (19) demonstrated no correlation between BMI and size conversion factor for the head. While a more practical approach might see age used to estimate the dose absorbed by patients, the variance is quite large (20). Head circumference (HC) is a vital brain index and has a standard pattern of growth development (21). Therefore, HC may serve as a potential indicator for estimating the absorbed dose (20). Shohji *et al.* (22) investigated the relationship between HC (measured with a band) and $SSDE_{293}$ using phantoms and clinical patients, although the sample size was too small to provide adequate statistical power. Moreover, only one scanner and single kilovoltage (kV) value were used in their research, while the conversion factor recommended in the AAPM report 293 results from integrating multiple kV values (14). However, the band performed with each patient may not be suitable for busy clinical work. To the best of our knowledge, a large sample with multiple scanners and multiple kV values that simultaneously explores the relationship between HC and $SSDE_{293}$ has not yet been reported.

Therefore, a large collection of head CT samples containing multiple kV values and scanners were selected for this study. We aimed to establish a simple and rapid method for estimating the radiation dose based on HC, eliminating the need for actual measurements of D_W for head CT examinations. We present the following article in accordance with the STROBE reporting checklist (available at https://qims.amegroups.com/article/view/10.21037/qims-22-983/rc).

Methods

Patients

Patients who underwent head CT at Union Hospital, Tongji Medical College, Huazhong University of Science and Technology and Hubei Cancer Hospital between December 2018 and September 2019 were retrospectively enrolled in this cross-sectional study. Patients with an incorrect head scan position, metal artifacts, hydrocephalus, microcephaly, and other congenital abnormalities of the brain and skull resulting in abnormal head size were excluded (n=119; *Figure 1*). The World Health Organization defines people under the age of 24 as young people (23). The data of patients younger than 24 years old were obtained from Union Hospital and the data from patients over 24 years old were from Hubei Cancer Hospital. Patient subgroups were then defined based on age into two groups: a younger group (<24 years; n=466) and an older group (≥24 years; n=756). Patient data were extracted from the picture archiving and communication system (PACS) and stored anonymously by scan ID, birth date, and scan date. This study was conducted

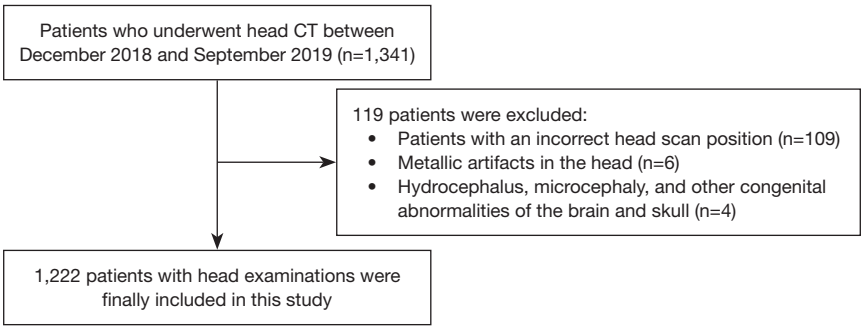

Figure 1 Flow diagram of the study population. CT, computed tomography.

in accordance with the Declaration of Helsinki (as revised in 2013) and was approved by the institutional review board of Tongji Medical College, Huazhong University of Science and Technology (No. 2021-IEC-A025). The need for written informed consent was waived due to the retrospective nature of the study.

Scan protocol

CT images were obtained using a 64-slice Siemens Definition AS+ (Siemens Healthcare, Erlangen, Germany) and GE Light Speed VCT (GE Healthcare Milwaukee, WI, USA). The parameters of the Siemens Definition AS+ were as follows: pitch, 0.55:1; care KV; care dose 4D (ref. mAs, 350 mAs); and rotation time, 1 s. The parameters of the GE Light speed VCT were as follows: pitch, 0.984:1; tube voltage, 100–120 kV; tube current, 150–400 mA; noise index, 2.8; and rotation time, 0.5 s. All patients were imaged in a supine position, and the scanning range was from the top to the base of the skull. The orbitomeatal baseline was employed as the scan reference line, whereas the circumference of the intermediate-level image was considered the HC.

Calculating D_W, f, and $SSDE_{293}$

The algorithms used for dose calculation were developed in MATLAB version 14 (Mathworks, Natick, Mass, USA) for the automated calculation of HC, D_W, *f*, and $SSDE_{293}$ from head CT images. First, the software selected the center slice of the scan volume for the images. We then converted the DICOM metadata to Hounsfield units (HU) and performed automatic patient contouring using an algorithm designed to produce accurate results with a relatively fast computation time. The algorithm combines basic segmentation techniques with specific information regarding the body boundaries of each patient. The specific algorithms are as follows: (I) segmentation of the human body region using the Otsu threshold segmentation algorithm and binarization operations; (II) filling of the cavity area of the segmented region through morphological expansion and corrosion operations (open and closed operation); (III) cutting off non-human regions such as the examination table by determining the number of segmented objects in the image by the size of the connected regions; and (IV) subjecting the binary images to edge extraction, extraction of human contours, and calculation of the perimeter and diameter of the human region. The built-in algorithm function in the MATLAB image processing toolkit toolbox was used for all steps in the algorithm (see Figure S1, Tables S1-S3). Ultimately, the largest identified area was considered the boundary of the patient. The efficiency of automated segmentation in the head was verified by the analysis of 30 randomly selected cases. The results showed the mean intersection over union (IoU) was 0.932, which was close to both that listed in the AAPM report 220 (12) (0.932), and that reported by Anam *et al.* (24) (0.927), and Juszczyk *et al.* (25) (0.975). The original image was then cropped using the results of the automatic contour, and its area and the average HU value were calculated. D_W was then calculated using Eq. [3].

To calculate the water-equivalent attenuation (A_W) and D_W, the following equations were used:

$$A_w = \sum\left(\frac{CT(x,y)}{1000}+1\right)\times A_{pxiel} \quad [1]$$

$$D_w = 2\times\sqrt{\frac{A_w}{\pi}} \quad [2]$$

$$D_w = 2\sqrt{\left[\frac{1}{1000}CT_{ROI}+1\right]\frac{A_{ROI}}{\pi}} \quad [3]$$

The conversion factor (f_{293}) calculation formula was as follows:

$$f_{293} = \alpha e^{-\beta D_w} \quad [4]$$

where:

$$\alpha = 1.9852\left[\text{absorbed dose to tissue}\,(\text{mGy})/\text{CTDI}_{\text{vol},16}\,(\text{mGy})\right] \quad [5]$$

$$\beta = 0.0486\left(cm^{-1}\right) \quad [6]$$

where D_w represents the water-equivalent diameter (cm), A_{ROI} is the area of the patient after cropping, and CT_{ROI} is the average HU value of the patient.

$SSDE_{293}$ was calculated using Eq. [7]

$$SSDE_{293} = f_{293} \times CTDI_{vol,16} \quad [7]$$

where f_{293} represents the $CTDI_{vol,16}$-to-$SSDE_{293}$ conversion factors for CT examinations of the head according to the AAPM report 293, and $CTDI_{vol,16}$ is the scanner-reported $CTDI_{vol}$.

Data analysis

Statistical analysis was performed using SPSS version 22.0 (IBM Corp. Armonk, NY, USA). Continuous variables are presented as the mean ± standard deviation if otherwise stated. The average age, conversion factor, and dose indices ($CTDI_{vol}$ and $SSDE_{293}$) were recorded for each patient per head CT examination, and the normality of variables was examined using a histogram. The relationship between age, HC, and the conversion factor $SSDE_{293}$ was evaluated using Pearson correlation coefficients (r). Values with $P \leq 0.05$ denoted statistical significance. The correlation interpretation (r) is as follows: $|r|=1$, perfect correlation; $0.8 \leq |r| < 1$, strong correlation; $0.5 \leq |r| < 0.8$, moderate correlation; $0.1 \leq |r| < 0.5$, weak correlation; and $0 < |r| < 0.1$, the lowest correlation (16). Missing data were examined, and no patterns of missing data were identified.

Results

Patient age and HC across subgroups

A total of 1,222 participants with a mean age of 40.79±24.68 years and range of 4 months to 90 years were retrospectively enrolled for $SSDE_{293}$ analysis. The data of age, HC, conversion factor, and SSDE grouped in this study conformed to a normal distribution. The mean HC was 53.17±2.95 cm, with a range of 35.52–64.89 cm. The overall mean $CTDI_{vol}$ and $SSDE_{293}$ were 54.53±8.73 and 46.92±8.23 mGy, respectively. The mean overall D_w and f_{293} were 17.25±0.96 cm and 0.86±0.04, respectively (*Table 1*).

With an increase in age, the HC gradually increased and reached the maximum value (55.42±2.44 cm) at 16–17 years old (*Table 2*). Simultaneously, the conversion factor (f_{293}) decreased gradually and reached a minimum value (0.83 of 0.03), while this and $SSDE_{293}$ gradually decreased with increasing HC. $SSDE_{293}$ reached the minimum value (44.86±6.40 mGy) at a HC of 55 cm.

Correlations between age, HC, $SSDE_{293}$, and f_{293}

Figure 2A shows a weak negative correlation between age and $SSDE_{293}$ in the younger group (r=–0.33; P<0.001), while a lower negative correlation was reported in the older group in *Figure 2B* (r=–0.12; P<0.001). A weak negative correlation between HC and $SSDE_{293}$ was seen in the younger group (*Figure 2C*) (r=–0.44; P<0.001), while in the older group, HC was not correlated with $SSDE_{293}$ (P=0.224; *Figure 2D*). In most cases, $SSDE_{293}$ was lower than the corresponding $CTDI_{vol}$ value, while neither age nor HC correlated with $CTDI_{vol}$.

Figure 3 shows the relationship between age, HC, and the conversion factor (f_{293}). The negative correlation between age and f_{293} in the younger group (r=–0.80; P<0.001; strong correlation) was higher than that in the older group (r=–0.13; P=0.001; weak correlation). Similarly, the negative correlation between HC and f_{293} in the younger group (r=–0.92; P<0.001; strong correlation) was higher than that in the older group (r=–0.82; P<0.001; strong correlation). Regardless of these findings, the negative correlation of the conversion factor with HC was better than that with age.

Discussion

The present study demonstrated a weak inverse correlation between age and HC with $SSDE_{293}$ in participants aged >24 years ($|r|<0.44$). HC exhibited a strong negative correlation with the conversion factor in both the younger and older age groups (r=–0.92 and –0.82, respectively).

Many studies have attempted to simplify the calculation of SSDE to achieve rapid dose estimation using various

Table 1 Summary of 1,222 head CT examinations with different age subgroups

Age subgroups (years)	Age (years)	D_w (cm)	HC (cm)	f_{293}	$CTDI_{vol}$ (mGy)	$SSDE_{293}$ (mGy)
Overall	40.79±24.68	17.25±0.96	53.17±2.95	0.86±0.04	54.53±8.73	46.92±8.23
0–1 (n=22)	0.55±0.51	14.00±1.21	44.52±3.63	1.01±0.06	62.39±2.49	62.78±3.92
2–3 (n=29)	2.38±0.49	15.18±0.72	47.86±2.52	0.95±0.03	59.15±9.81	56.20±9.63
4–5 (n=49)	4.49±0.51	15.84±0.43	49.64±2.58	0.92±0.02	60.22±8.91	55.40±8.32
6–7 (n=35)	6.46±0.51	16.17±0.66	50.45±2.37	0.91±0.03	63.38±0.75	57.37±1.79
8–9 (n=46)	8.48±0.51	16.38±0.49	50.84±1.47	0.90±0.02	61.74±5.55	55.27±4.93
10–11 (n=34)	10.47±0.51	16.65±0.52	51.89±1.64	0.88±0.02	62.47±5.27	55.23±4.88
12–13 (n=42)	12.43±0.50	17.30±0.59	53.68±1.83	0.86±0.02	60.55±8.66	51.90±7.65
14–15 (n=35)	14.43±0.50	17.42±0.53	54.51±2.72	0.85±0.02	63.69±0.71	54.24±1.36
16–17 (n=38)	16.34±0.48	17.88±0.70	55.42±2.44	0.83±0.03	63.73±0.43	53.09±1.88
18–19 (n=42)	18.48±0.51	17.77±0.53	54.96±2.06	0.84±0.02	62.21±6.55	52.07±5.57
20–29 (n=104)	22.52±2.15	17.93±0.75	55.04±2.89	0.83±0.03	62.64±3.43	52.04±3.32
30–39 (n=43)	35.53±2.52	17.68±0.56	53.71±1.99	0.84±0.02	51.10±5.69	42.96±4.78
40–49 (n=132)	45.84±2.61	17.51±0.51	53.27±2.05	0.85±0.02	50.62±6.34	42.93±5.48
50–59 (n=220)	54.77±2.64	17.50±0.60	53.72±2.18	0.85±0.02	50.14±6.71	42.54±5.80
60–69 (n=209)	64.31±2.78	17.45±0.62	53.73±2.15	0.85±0.03	49.54±6.52	42.11±5.53
70–79 (n=114)	73.82±2.87	17.45±0.61	53.76±1.89	0.85±0.03	48.42±6.85	41.14±5.72
≥80 (n=28)	83.14±2.72	17.19±0.74	52.99±1.93	0.86±0.03	46.74±8.03	40.19±6.68

Data are presented as the means ± standard deviations. D_w, water-equivalent diameter; HC, head circumference; f_{293}, conversion factors; $CTDI_{vol}$, volumetric computed tomography dose index; $SSDE_{293}$, specific size dose estimation.

methods, such as using a suitable body shape (AP, LAT, D_{eff}, etc.) or age to characterize SSDE (18,26,27). Kritsaneepaiboon *et al.* (17) demonstrated a higher correlation between body weight and SSDE than between age and SSDE. Notably, the lowest variability was calculated at less than 20 kg of body weight and <4 years of age. The patient's weight, as a readily available measurement method from clinical records, may offer a quick and simple approach for pediatric SSDE measurements (18). Similarly, age can be used with body size parameters from the ICRU 74 report to approximate the effective diameter, although this does not account for variations in body habitus. Cheng *et al.* (28) demonstrated a satisfactory correlation between body size and age in the torso region, and normalization coefficients employing different phantoms revealed the mean absolute percentage error was less than 2.3%. In our study, the correlation coefficient of HC with $SSDE_{293}$ (r=–0.44) was lower than that with f_{293} (r=–0.92). These results show f_{293} can be calculated using a conversion formula, such that f_{293} = a × HC + b (where a and b are constants), whereas the calculation formula for $SSDE_{293}$ is known ($SSDE_{293} = f_{293} \times CTDI_{vol}$) (14). Therefore, $SSDE_{293}$ can be converted to the following equation: $SSDE_{293} = a \times HC \times CTDI_{vol} + b \times CTDI_{vol}$. As shown, both HC and $CTDI_{vol}$ affected the $SSDE_{293}$ result, which may explain the difference in the correlation coefficients between HC with $SSDE_{293}$ and f_{293}.

The conversion factor is a crucial parameter for calculating SSDE. Previously, Alikhani *et al.* (19) showed BMI was not significantly correlated with the conversion factor of the head, and tended to be constant with an increase in BMI. Therefore, it is not feasible to use body weight or BMI to rapidly estimate SSDE. Our present study revealed a strong negative correlation between HC and the conversion factor (r=–0.92) in the younger group, which could be explained by understanding the general growth pattern of children. Collectively, as a child grows, the HC is more relevant than body weight, making it a crucial indicator of growth and development and a feature

Table 2 Summary of 1,222 head CT examinations with different HC subgroups

HC subgroups (cm)	Age (years)	D_w (cm)	HC (cm)	f_{293}	$CTDI_{vol}$ (mGy)	$SSDE_{293}$ (mGy)
≤41 (n=4)	0.50±1.00	12.01±0.94	38.18±2.49	1.11±0.05	60.86±5.18	67.53±7.35
42 (n=3)	0.00	13.25±0.07	42.26±0.11	1.04±0.00	60.38±2.35	62.96±2.55
43 (n=2)	1.00±1.41	13.80±0.27	43.50±0.53	1.02±0.01	63.10±1.23	64.06±0.41
44 (n=2)	4.00±4.24	14.31±0.39	44.52±0.27	0.99±0.02	63.21±0.93	62.61±2.12
45 (n=8)	1.50±1.07	14.41±0.20	45.60±0.20	0.99±0.01	62.94±0.97	62.04±1.42
46 (n=14)	2.14±1.56	14.70±0.26	46.47±0.32	0.97±0.01	60.53±8.27	58.83±8.15
47 (n=16)	7.25±13.46	15.29±0.24	47.54±0.37	0.94±0.01	59.84±6.18	56.52±5.99
48 (n=25)	10.40±17.76	15.62±0.22	48.57±0.34	0.93±0.01	59.72±8.51	55.52±8.06
49 (n=58)	21.36±26.29	16.01±0.28	49.48±0.27	0.91±0.01	54.49±13.04	49.73±12.06
50 (n=90)	33.02±27.44	16.43±0.30	50.53±0.31	0.89±0.01	56.46±8.57	50.49±8.00
51 (n=139)	42.63±23.35	16.84±0.26	51.58±0.27	0.88±0.01	53.14±9.18	46.55±8.16
52 (n=215)	44.86±21.27	17.16±0.28	52.49±0.28	0.86±0.01	53.08±8.72	45.79±7.73
53 (n=199)	48.73±22.10	17.42±0.30	53.48±0.29	0.85±0.01	53.15±8.21	45.27±7.16
54 (n=148)	46.49±22.52	17.73±0.26	54.47±0.28	0.84±0.01	53.77±8.32	45.12±7.12
55 (n=126)	48.27±21.73	18.00±0.31	55.41±0.28	0.83±0.01	54.19±7.61	44.86±6.40
56 (n=93)	43.59±21.46	18.30±0.35	56.47±0.30	0.82±0.01	55.25±7.46	45.07±6.14
57 (n=35)	42.40±21.20	18.53±0.40	57.51±0.32	0.81±0.02	56.89±6.80	45.89±5.49
58 (n=19)	33.79±19.34	18.55±0.72	58.54±0.28	0.81±0.03	57.41±9.40	46.26±7.57
59 (n=13)	29.54±16.76	18.44±0.92	59.54±0.29	0.81±0.04	60.82±5.78	49.26±4.57
≥60 (n=13)	31.92±20.36	18.09±1.07	62.71±2.62	0.83±0.04	57.23±9.10	47.07±7.04

Data are presented as the means ± standard deviations. D_w, water-equivalent diameter; HC, head circumference; f_{293}, conversion factors; $CTDI_{vol}$, volumetric computed tomography dose index; $SSDE_{293}$, specific size dose estimation.

of patient size. Fahmi *et al.* (29) also reported a satisfactory correlation between age and head diameter in pediatric patients during head CT examinations, and the correlation coefficient for female patients was as high as 0.94. Our study also showed a stronger negative correlation (r=–0.80) between age and the conversion factor, with both age groups showing stronger correlation coefficients between HC and the conversion factor than between age and the conversion factor. Typically, HC increases with age, specifically in the pediatric population, and evidence from a previous study demonstrated a rapid increase in HC before the age of 5 years and decline thereafter (30). In the present study, age was independent of conversion factors after adulthood, and the correlation between age and conversion factors was relatively low. In contrast, HC exhibited a satisfactory negative correlation with the conversion factors in adolescent patients. It is possible to rapidly estimate the patient's absorbed dose during a clinical head examination by rapidly acquiring the HC measurement. $SSDE_{293}$ estimation based on HC and age potentially saves a significant amount of time compared to the tedious method of measuring AP, LAT, and D_W thickness using calipers. Thus, a major advantage of this method is the reliable estimation of the expected absorbed dose before image acquisition (19,30). Moreover, the ability to calculate the expected patient dose before image acquisition undoubtedly provides valuable additional insights for optimizing X-ray safety in CT examinations, as the absorbed dose that follow-up patients may receive can be evaluated more quickly and accurately by HC before examination. These findings will guide radiology technologists in selecting the appropriate parameters during scanning to ensure the patient's absorbed

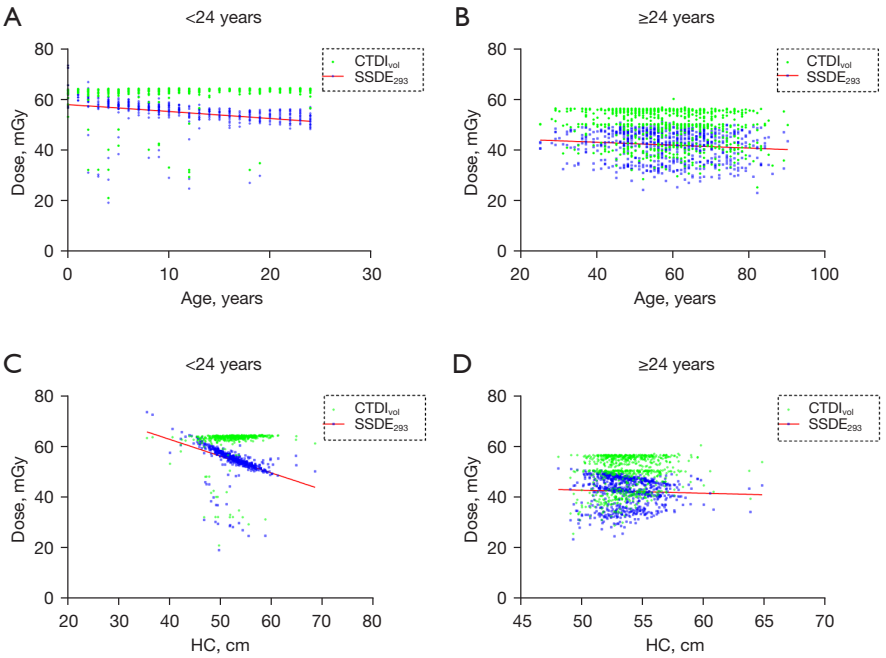

Figure 2 Graphs of $SSDE_{293}$ as a function of age and HC for different age groups. (A) Association of $SSDE_{293}$ and $CTDI_{vol}$ with age in younger age groups; (B) association of $SSDE_{293}$ and $CTDI_{vol}$ with age in older age groups; (C) association of $SSDE_{293}$ and $CTDI_{vol}$ with HC in younger age groups; (D) association of $SSDE_{293}$ and $CTDI_{vol}$ with HC in older age groups. $SSDE_{293}$, specific size dose estimation; HC, head circumference; $CTDI_{vol}$, volumetric computed tomography dose index.

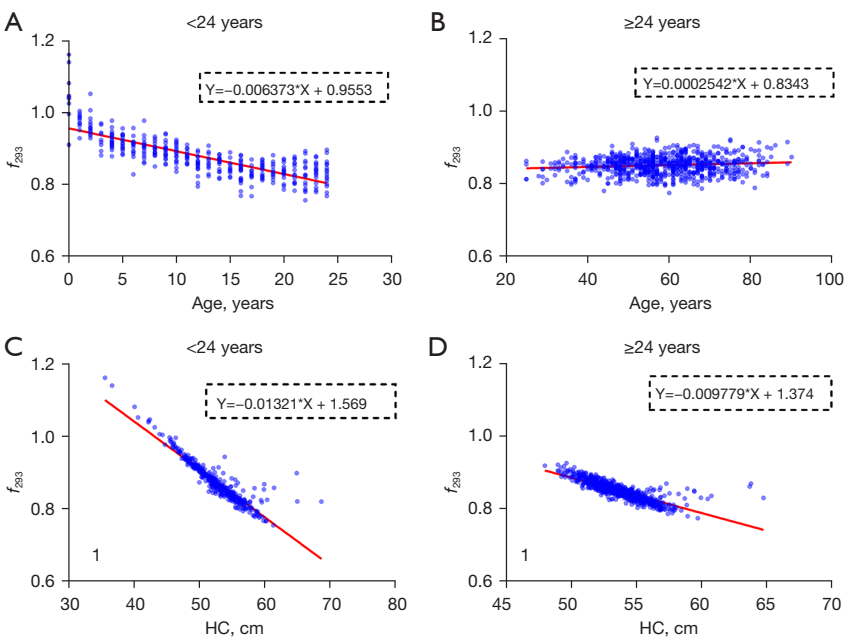

Figure 3 Graphs of f_{293} as a function of age and HC for different age groups. (A) Linear relationship between f_{293} and age in the younger group; (B) linear relationship between f_{293} and age in the older group; (C) linear relationship between f_{293} and HC in the younger group; (D) linear relationship between f_{293} and HC in the older group. The equation in the figure is the equation of f_{293} and HC, where X denotes the HC, while Y denotes the conversion factor (*f* factor). f_{293}, conversion factors; HC, head circumference.

dose is within the prescribed dose.

This study has some limitations that warrant further investigation. First, the number of patients aged 18–24 years old (n=136) and infants (n=10) was small. As such, insufficient samples were analyzed in this age group, which contributed to a decrease in the correlation coefficient. Meanwhile, there was no sex subgroup study, which may also lead to a low correlation coefficient between the conversion factor, HC, and age. Future analyses using larger sample sizes are necessary to better represent the relevant population. Second, the automatic sketching software only extracted the middle layer of the scanning image and could not completely replace the measurement of clinical HC. Finally, the conversion factor under a single kV in the AAPM report 293 was not used for the calculation because the applied conversion factor was comprehensive. The use of a single scanner, scanning protocol, and parameters to achieve ideal experimental results are possible research directions for subsequent experiments. Therefore, further investigations are warranted in future studies.

In conclusion, HC in patients was associated with the head conversion factor. The correlation coefficient of HC with the conversion factor was better than that of $SSDE_{293}$. It is feasible to quickly estimate the absorbed dose of head CT examinations based on HC using the AAPM report 293.

Acknowledgments

Funding: This study was supported by the National Natural Science Foundation of China (No. 62076257) and the Applied Basic Research Program of Wuhan (No. 2020020601012239).

Footnote

Reporting Checklist: The authors have completed the STROBE reporting checklist. Available at https://qims.amegroups.com/article/view/10.21037/qims-22-983/rc

Conflicts of Interest: All authors have completed the ICMJE uniform disclosure form (available at https://qims.amegroups.com/article/view/10.21037/qims-22-983/coif). The authors have no conflicts of interest to declare.

Ethical Statement: The authors are accountable for all aspects of the work in ensuring that questions related to the accuracy or integrity of any part of the work are appropriately investigated and resolved. This study was conducted in accordance with the Declaration of Helsinki (as revised in 2013) and was approved by the institutional review board of Tongji Medical College, Huazhong University of Science and Technology (No. 2021-IEC-A025). The need for written informed consent was waived due to the retrospective nature of the study.

References

1. Kanal KM, Butler PF, Sengupta D, Bhargavan-Chatfield M, Coombs LP, Morin RL. U.S. Diagnostic Reference Levels and Achievable Doses for 10 Adult CT Examinations. Radiology 2017;284:120-33.
2. Mihailidis D, Tsapaki V, Tomara P. A simple manual method to estimate water-equivalent diameter for calculating size-specific dose estimate in chest computed tomography. Br J Radiol 2021;94:20200473.
3. Khatonabadi M, Kim HJ, Lu P, McMillan KL, Cagnon CH, DeMarco JJ, McNitt-Gray MF. The feasibility of a regional CTDIvol to estimate organ dose from tube current modulated CT exams. Med Phys 2013;40:051903.
4. Rawashdeh M, Saade C, Zaitoun M, Abdelrahman M, Brennan P, Alewaidat H, McEntee MF. Establishment of diagnostic reference levels in cardiac computed tomography. J Appl Clin Med Phys 2019;20:181-6.
5. Satharasinghe DM, Jeyasugiththan J, Wanninayake WMNMB, Pallewatte AS. Paediatric diagnostic reference levels in computed tomography: a systematic review. J Radiol Prot 2021. [Epub ahead of print]. doi: 10.1088/1361-6498/abd840.
6. McCollough CH, Leng S, Yu L, Cody DD, Boone JM, McNitt-Gray MF. CT dose index and patient dose: they are not the same thing. Radiology 2011;259:311-6.
7. Li Y, Jiang Y, Liu H, Yu X, Chen S, Ma D, Gao J, Wu Y. A phantom study comparing low-dose CT physical image quality from five different CT scanners. Quant Imaging Med Surg 2022;12:766-80.

8. Ha JY, Baek HJ, Ryu KH, Cho E. Feasibility study of ultra-low-dose dedicated maxillofacial computed tomography using filter-based spectral shaping in patients with craniofacial trauma: assessment of image quality and radiation dose. Quant Imaging Med Surg 2021;11:1292-302.
9. Kalender WA. Dose in x-ray computed tomography. Phys Med Biol 2014;59:R129-50.
10. Tabesh J, Mahdavi M, Haddadi G, Ravanfar Haghighi R, Jalli R. Determination of Diagnostic Reference Level (DRL) in Common Computed Tomography Examinations with the Modified Quality Control-Based Dose Survey Method in Four University Centers: A Comparison of Methods. J Biomed Phys Eng 2021;11:447-58.
11. Leng S, Shiung M, Duan X, Yu L, Zhang Y, McCollough CH. Size-specific Dose Estimates for Chest, Abdominal, and Pelvic CT: Effect of Intrapatient Variability in Water-equivalent Diameter. Radiology 2015;276:184-90.
12. McCollough C, Bakalyar DM, Bostani M, Brady S, Boedeker K, Boone JM, Chen-Mayer HH, Christianson OI, Leng S, Li B, McNitt-Gray MF, Nilsen RA, Supanich MP, Wang J. Use of Water Equivalent Diameter for Calculating Patient Size and Size-Specific Dose Estimates (SSDE) in CT: The Report of AAPM Task Group 220. AAPM Rep 2014;2014:6-23.
13. Boone JM. Reply to "Comment on the 'Report of AAPM TG 204: Size-specific dose estimates (SSDE) in pediatric and adult body CT examinations'" [AAPM Report 204, 2011]. Med Phys 2012;39:4615-6.
14. McCollough C, Bakalyar DM, Bostani M, Brady S, Boedeker K, Boone JM, Chen-Mayer HH, Christianson OI, Leng S, Li B, McNitt-Gray MF, Nilsen RA, Supanich MP, Wang J. Use of Water Equivalent Diameter for Calculating Patient Size and Size-Specific Dose Estimates (SSDE) in CT: The Report of AAPM Task Group 220. AAPM Rep 2014;2014:6-23.
15. Hardy AJ, Bostani M, Hernandez AM, Zankl M, McCollough C, Cagnon C, Boone JM, McNitt-Gray M. Estimating a size-specific dose for helical head CT examinations using Monte Carlo simulation methods. Med Phys 2019;46:902-12.
16. Anam C, Kusuma Dewi W, Masdi M, Haryanto F, Fujibuchi T, Dougherty G. Investigation of Eye Lens Dose Estimate based on AAPM Report 293 in Head Computed Tomography. J Biomed Phys Eng 2021;11:563-72.
17. Kritsaneepaiboon S, Eng-Chuan S, Yoykaew S. Can Patient's Body Weight Represent Body Diameter for Pediatric Size-Specific Dose Estimate in Thoracic and Abdominal Computed Tomography? J Clin Imaging Sci 2019;9:24.
18. Khawaja RD, Singh S, Vettiyil B, Lim R, Gee M, Westra S, Kalra MK. Simplifying size-specific radiation dose estimates in pediatric CT. AJR Am J Roentgenol 2015;204:167-76.
19. Alikhani B, Getzin T, Kaireit TF, Ringe KI, Jamali L, Wacker F, Werncke T, Raatschen HJ. Correlation of size-dependent conversion factor and body-mass-index using size-specific dose estimates formalism in CT examinations. Eur J Radiol 2018;100:130-4.
20. Honorio da Silva E, Baffa O, Elias J Jr, Buls N. Conversion factor for size specific dose estimation of head CT scans based on age, for individuals from 0 up to 18 years old. Phys Med Biol 2021.
21. Onis MD , Who GE . WHO child growth standards: head circumference-for-age, arm circumference-for-age, triceps skin fold-for-age and sub scapular skin fold-for-age. J Trop Pediatr 2008;54:214-215.
22. Shohji T, Kuriyama K, Yanano N, Maeda E, Katoh Y. Simple method of measuring ssde for head CT: facilitating pre-CT scan dose calculation using specialized head scan band. Radiat Prot Dosimetry 2021;197:1-11.
23. Adolescent and Young Adult Health Unit. Available online: https://www.who.int/teams/maternal-newborn-child-adolescent-health-and-ageing/adolescent-and-young-adult-health
24. Anam C, Haryanto F, Widita R, Arif I, Dougherty G. Automated Calculation of Water-equivalent Diameter (DW) Based on AAPM Task Group 220. J Appl Clin Med Phys 2016;17:320-33.
25. Juszczyk J, Badura P, Czajkowska J, Wijata A, Andrzejewski J, Bozek P, Smolinski M, Biesok M, Sage A, Rudzki M, Wieclawek W. Automated size-specific dose estimates using deep learning image processing. Med Image Anal 2021;68:101898.
26. Brady SL, Kaufman RA. Investigation of American Association of Physicists in Medicine Report 204 size-specific dose estimates for pediatric CT implementation. Radiology 2012;265:832-40.
27. Menke J. Comparison of different body size parameters for individual dose adaptation in body CT of adults. Radiology 2005;236:565-71.
28. Cheng PM, Vachon LA, Duddalwar VA. Automated pediatric abdominal effective diameter measurements versus age-predicted body size for normalization of CT dose. J Digit Imaging 2013;26:1151-5.
29. Fahmi A, Anam C, Suryono S, Ali MH, Jauhari A.

Correlation between age and head diameters in the paediatric patients during CT examination of the head. Pol J Med Phys Eng 2019;25:229-35.

30. Schmidt B, Saltybaeva N, Kolditz D, Kalender WA. Assessment of patient dose from CT localizer radiographs. Med Phys 2013;40:084301.

Cite this article as: Chen T, Kong X, Peng W, Liao T, Hu H, Pan N, Yuan Z. Applying the AAPM 293 report to estimate the absorbed dose during head computed tomography: using head circumference for rapid dose estimation. Quant Imaging Med Surg 2023;13(5):3140-3149. doi: 10.21037/qims-22-983

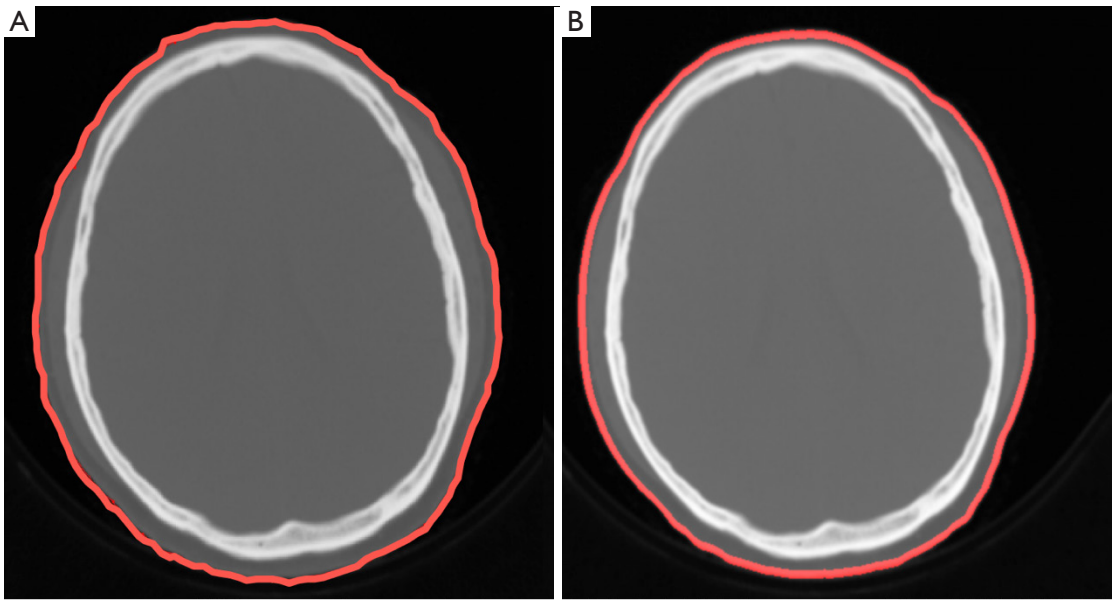

Figure S1 The schematic diagram of manual and automatic segmentation. (A) Manual segmentation diagram; (B) automatic segmentation diagram. Manual segmentation diagram software used ITK-SNAP (ITK-snap v.3.6.0, www.itksnap.org).

Table S1 The built-in function of Matlab image processing toolkits

Matlab function	Description
Otsuthresh	Computes a global threshold T from histogram counts
Imbinarize	Creates a binary image
Imerode	Erodes the binary image
Bwconncomp	Computes the connected components in the binary image
Bwperim	Find perimeter of objects in binary image
Regionprops	Measure properties of image segmentation regions

https://dx.doi.org/10.21037/qims-22-983

Table S2 IoU for automatic and manual segmentation

ID	Area	HC	CT value	IoU
100434	235.2294259	54.63482227	231.2670659	0.937279549
101652	212.4209017	51.82365511	205.6247417	0.943313722
103022	238.5131715	55.13717923	156.1267024	0.913737234
106420	209.6066713	51.69372353	213.4547482	0.936011289
107909	238.3226049	54.82854063	157.8132008	0.93592122
108025	222.528647	53.21725791	143.9216496	0.925378936
108038	254.7163143	57.17223635	182.6967336	0.916655704
108067	249.6827072	56.62169953	169.1432652	0.92729985
108143	217.4139777	53.27409382	115.7944284	0.955479711
108539	213.4359944	52.45164176	113.9499233	0.930215077
108893	235.4966681	54.88211739	134.1399536	0.963593629
108917	222.3116931	55.03362408	187.6061253	0.916185822
109437	207.4120305	51.17643864	133.3972212	0.922616489
111887	191.1196712	49.45320332	130.3826922	0.941361953
112426	249.4481632	56.33688522	138.7411017	0.937372133
114178	224.6970618	53.55490422	146.0388891	0.935239008
115351	216.6311447	52.46496843	137.8463451	0.912845285
115750	228.9346496	55.7125203	167.1628251	0.938344906
117124	226.0646606	53.61414141	184.8654336	0.936142707
118214	216.1429099	52.76247299	160.0462983	0.925106427
73236	215.6291022	52.521675	163.1829102	0.947971438
80967	210.6414795	51.53988281	121.1563179	0.934774516
88568	238.0468551	54.93943945	190.0891825	0.914513565
90619	218.1581409	52.59176995	194.8105564	0.944616308
92368	251.2158544	56.38776782	171.8879451	0.917890583
95248	227.4594362	53.61628114	200.8641126	0.939316282
97933	210.1919883	51.68512979	164.3800277	0.944680851
99308	211.2344725	51.92302029	142.8295107	0.926335975
99481	231.0309429	54.06940591	169.5942259	0.930822549
99914	274.8647498	58.91149327	153.3557636	0.918181421
Average				0.932306805

IoU, intersection over union; HC, head circumference; CT, computed tomography.

https://dx.doi.org/10.21037/qims-22-983

Table S3 Comparison of segmentation efficiency metrics obtained using the approaches suggested by AAPM [2014] (report 220), by Anam *et al*. [2016], Juszczyk *et al.* [2020] and by our method

Method	Average IoU
AAPM report 220 (AAPM, 2014)	0.9320
Anam *et al*. [2016]	0.9269
Juszczyk *et al*. [2020]	0.9752
Our method	0.9323

AAPM, The American Association of Physicists in Medicine; IoU, intersection over union.

https://dx.doi.org/10.21037/qims-22-983